

Optimized Dual-Trajectory Tracking Control of a 9-DoF WMRA System for ADL Tasks

F. Farelo, R. Alqasemi, and R. Dubey

Abstract—Wheelchair-bound persons with upper limb motion limitations can utilize a wheelchair-mounted robotic arm (WMRA) to perform activities of daily living (ADL) tasks. In this paper, an optimized control of our 9-DoF system, consisting of a 7-DoF robotic arm and a 2-DoF power wheelchair, is achieved. For effective ADL task execution, positioning the end-effector with proper wheelchair orientation was optimized as part of the control algorithm. Separate wheelchair and end-effector trajectories were simultaneously followed to execute a “Go To and Open the Door” task. The control methodology, implementation and test results in simulation are presented in this paper.

Index Terms – Dual-Trajectory, Mobile Robot, Manipulator, redundancy, ADL

I. INTRODUCTION

According to the latest available data from the US Census Bureau [1], about 54.4 million Americans had some level of disability, 34.9 million of them had a severe disability. About 11 million Americans older than 6 years of age needed personal assistance with one or more activities of daily living (ADL). This work focuses on people with limited upper and lower extremity mobility due to spinal cord injury or dysfunction, or genetic predispositions. Robotic aides used in these applications vary from advanced limb orthosis to robotic arms [2]. A wheelchair mounted robotic arm can enhance the manipulation capabilities of individuals with disabilities that are using power wheelchairs, and reduce dependence on human aides.

Two prototypes of the wheelchair-mounted robotic arm (WMRA) have been designed and developed to enhance the capabilities of mobility-impaired persons with limited upper extremities limitations exceeding previous models specifications and performance [3, 4]. The combination of the wheelchair mobility and the arm manipulation in an optimized redundancy resolution algorithm [3] allowed for the possibility of programming pre-set ADL tasks to be autonomously executed. Some ADL tasks, such as “Go To and Open the Door” task, require wheelchair orientation

control to place the WMRA in a configuration that makes the task possible. In this context, having a secondary trajectory for the wheelchair to follow while the arm is following its main trajectory allows for an easier task execution.

This work utilizes redundancy to control 2 separate trajectories, a primary trajectory for the end-effector and an optimized secondary trajectory for the wheelchair. Even though this work presents results and implementation in the WMRA virtual reality simulation environment, this approach offers expandability to many wheeled base mobile manipulators in different types of applications.

II. BACKGROUND

Redundant mobile manipulators as a research topic has gained interest with its potential for a wide range of applications. In [5], a 7 DoF mobile manipulator consisting of a 5 DoF arm mounted on a 2 DoF wheeled platform was controlled by coordinating the platform motion and the gripper motion. The platform was driven to a destination that put the target within the gripper’s workspace.

The non-holonomic wheeled platform of manipulators was addressed in [6], where redundancy for a planar mobile manipulator was resolved using extended reduced gradient and projected gradient optimization-based methods. This approach was tested in simulation by having the end effector pointing at a pre-specified orientation while the wheelchair followed a circular trajectory, however they did not attempt to control two separate trajectories for the end effector and the non-holonomic base.

Path planning for non-holonomic mobile robots has been addressed by researchers for more than 2 decades. In [7], this was implemented for obstacle avoidance and implemented using the non-holonomic constrains of the platform. However, combining this constrains with a redundant manipulator was not considered at that time. In [8], an on-line planner for obstacle avoidance with moving targets was presented. Their model is suitable for real time generation of trajectories and it was tested in crowded simulated environments.

Recent work in redundancy resolution of mobile robots has accomplished the task of sustaining separate trajectories for the end effector and the platform. In [9] they implemented redundancy resolution of a 2D mobile manipulator using independent controllers developed within each other’s decoupled space, which facilitated the redundancy resolution at a dynamic level. The separate trajectories will be controlled by extending the weighted

Manuscript received September 15, 2009. This work was supported in part by the National Science Foundation (NSF) under Grant IIS-0713560.

Fabian Farelo is with the University of South Florida, Tampa, FL 33620, USA. (phone: 813-974-2115; fax: 813-974-3539; e-mail: ffarelo@mail.usf.edu).

Redwan Alqasemi is with the University of South Florida, Tampa, FL 33620, USA. (e-mail: ralqasemi@gmail.com).

Rajiv Dubey is with the University of South Florida, Tampa, FL 33620, USA. (e-mail: Dubey@eng.usf.edu)

least norm solution method [10] to constrain or prioritize the motion of the platform to follow certain trajectories. This method was intended for resolving redundancy while minimizing unnecessary motion of the joints. This approach has also been used along with specific criterion functions to avoid joint limits [11].

In this work, we develop and optimize a control system that combines the manipulation of the robotic arm and the mobility of the wheelchair in a single control algorithm. Redundancy resolution is to be optimally solved to avoid singularities and joint limits. While the end-effector follows a primary trajectory, we introduce a secondary trajectory to be followed by the wheelchair as part of the redundancy resolution and optimization algorithm.

III. DUAL-TRAJECTORY CONTROL

A. WMRA combined Kinematics

Two of the DoFs are provided by the non-holonomic motion of the wheelchair. This subsystem is controlled using 2 input variables: the linear position of the wheelchair along its x-axis, and the angular position of the wheelchair about its z-axis (see figure 1). The planar motion of the wheelchair includes three variables: the x and y positions, and the z-orientation of the wheelchair [12].

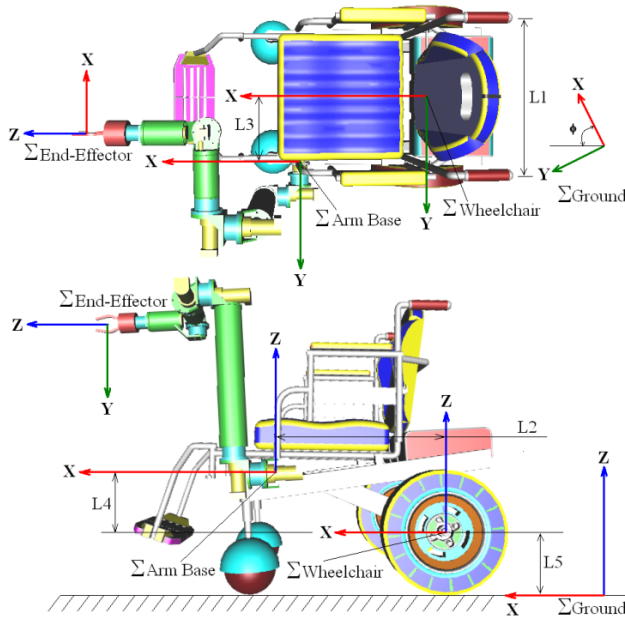


Figure 1. WMRA coordinate frames

Assuming that the manipulator is mounted on the wheelchair with L2 and L3 offset distances from the center of the differential drive across the x and y coordinates respectively (see figure 1), the mapping of the wheels' velocities to the manipulator's end effector velocities along its coordinates is defined by:

$$\dot{\mathbf{r}}_c = \mathbf{J}_c \cdot \mathbf{J}_w \cdot \mathbf{V}_c \quad (1)$$

where \mathbf{J}_c and \mathbf{J}_w are the jacobians that map the end-effector velocities to the arm base velocities (without arm motion) and the arm base velocities to the wheels' velocities

respectively and the end effector velocity and manipulator velocity are:

$$\dot{\mathbf{r}}_c = \begin{bmatrix} \dot{x} & \dot{y} & \dot{z} & \dot{\alpha} & \dot{\beta} & \dot{\phi} \end{bmatrix}^T, \quad \mathbf{V}_c = \begin{bmatrix} \dot{\theta}_l \\ \dot{\theta}_r \end{bmatrix}, \text{ and}$$

$$\mathbf{J}_c = \begin{bmatrix} \mathbf{I}_{2 \times 2} & \begin{bmatrix} -(\mathbf{P}_{xg} \cdot \mathbf{S}\phi + \mathbf{P}_{yg} \cdot \mathbf{C}\phi) \\ \mathbf{P}_{xg} \cdot \mathbf{C}\phi - \mathbf{P}_{yg} \cdot \mathbf{S}\phi \end{bmatrix} \\ \mathbf{0}_{2 \times 2} & \mathbf{0}_{3 \times 1} \\ \mathbf{0}_{2 \times 2} & \mathbf{I} \end{bmatrix}_{6 \times 3},$$

$$\mathbf{J}_w = \frac{1}{2} \begin{bmatrix} c\phi_c + \frac{2}{l_1}(l_2 s\phi_c + l_3 c\phi_c) & c\phi_c - \frac{2}{l_1}(l_2 s\phi_c + l_3 c\phi_c) \\ s\phi_c - \frac{2}{l_1}(l_2 c\phi_c - l_3 s\phi_c) & s\phi_c + \frac{2}{l_1}(l_2 c\phi_c - l_3 s\phi_c) \\ -\frac{2}{l_1} & \frac{2}{l_1} \end{bmatrix}_{3 \times 2}$$

where \mathbf{P}_{xg} and \mathbf{P}_{yg} are the x-y coordinates of the end-effector based on the arm base frame, ϕ is the angle of the arm base frame, which is the same as the angle of the wheelchair based on the ground frame, and L5 is the wheels' radius. The above Jacobian can be used to control the wheelchair with the Jacobian of the arm after combining them together.

The wheelchair will move forward when both wheels have the same speed and direction while rotational motion will be created when both wheels rotate at the same velocity but in opposite directions. Since the wheelchair's position and orientation are our control variables rather than the left and right wheels' velocities, \mathbf{V}_c can be redefined as:

$$\mathbf{V}_c = \begin{bmatrix} \dot{X} \\ \dot{\phi} \end{bmatrix}, \text{ where: } \dot{\phi} = \frac{2l_5 \dot{\theta}_r}{l_1}, \text{ and } \dot{X} = l_5 \dot{\theta}_r$$

Seven DoFs are provided by the robotic arm mounted on the wheelchair. From the DH parameters of the robotic arm specified in earlier publications [13], the 6x7 Jacobian that relates the joint rates to the Cartesian speeds of the end effector based on the base frame is generated according to Craig's notation [14]:

$$\dot{\mathbf{r}}_A = \mathbf{J}_A \cdot \mathbf{V}_A \quad (2)$$

where: $\dot{\mathbf{r}}_A = \begin{bmatrix} \dot{x} & \dot{y} & \dot{z} & \dot{\alpha} & \dot{\beta} & \dot{\gamma} \end{bmatrix}^T$ is the task vector, and $\mathbf{V}_A = \begin{bmatrix} \dot{\theta}_1 & \dot{\theta}_2 & \dot{\theta}_3 & \dot{\theta}_4 & \dot{\theta}_5 & \dot{\theta}_6 & \dot{\theta}_7 \end{bmatrix}^T$ is the joint rate vector, and \mathbf{J}_A is the robotic arm's Jacobian.

Combining the wheelchair and arm kinematics yields the total system kinematics. In the case of combined control, let the task vector be:

$$\mathbf{r} = \mathbf{f}(q_c, q_A) \quad (3)$$

where q_c and q_A are the control variables of the wheelchair and arm respectively. Differentiating (3) with respect to time gives:

$$\dot{\mathbf{r}} = \frac{\partial \mathbf{f}}{\partial q_c} \mathbf{V}_c + \frac{\partial \mathbf{f}}{\partial q_A} \mathbf{V}_A = \mathbf{J}_c \mathbf{J}_w \mathbf{V}_c + \mathbf{J}_A \mathbf{V}_A = \begin{bmatrix} \mathbf{J}_A & \mathbf{J}_c \mathbf{J}_w \end{bmatrix} \begin{bmatrix} \mathbf{V}_A \\ \mathbf{V}_c \end{bmatrix},$$

or,

$$\dot{\mathbf{r}} = \mathbf{J} \cdot \mathbf{V} \quad (4)$$

where: $\dot{\mathbf{r}} = \begin{bmatrix} \dot{x} & \dot{y} & \dot{z} & \dot{\alpha} & \dot{\beta} & \dot{\phi} \end{bmatrix}^T$, $\mathbf{J} = \begin{bmatrix} \mathbf{J}_A & \mathbf{J}_c \mathbf{J}_w \end{bmatrix}$, and

$$V = [V_A \quad V_c]^T = [\dot{\theta}_1 \quad \dot{\theta}_2 \quad \dot{\theta}_3 \quad \dot{\theta}_4 \quad \dot{\theta}_5 \quad \dot{\theta}_6 \quad \dot{\theta}_7 \quad \dot{X} \quad \dot{\varphi}]^T.$$

B. Redundancy resolution and optimization

Redundancy is resolved in the algorithm using S-R inverse of the Jacobian [15] to give a better approximation around singularities, and use the optimization for different subtasks. Manipulability measure [16] is used as a factor to measure how far is the current configuration from singularity. This measure is defined as $w = \sqrt{\det(J^*J^T)}$. The S-R Inverse of the Jacobian in this case is defined as:

$$\underline{J}^* = \underline{J}^T * (\underline{J} * \underline{J}^T + k * \underline{I}_6)^{-1} \quad (5)$$

where \underline{I}_6 is a 6x6 identity matrix, and k is a scale factor. It has been known that this method reduces the joint velocities near singularities, but compromises the accuracy of the solution by increasing the joint velocities error. Choosing the scale factor k is critical to minimize the error. Since the point in using this factor is to give approximate solution near and at singularities, an adaptive scale factor is updated at every time step to put the proper factor as needed:

$$k = \begin{cases} k_0 * (1 - \frac{w}{w_0})^2 & \text{for } w < w_0 \\ 0 & \text{for } w \geq w_0 \end{cases}, \quad (6)$$

where w_0 is the manipulability measure at the start of the boundary chosen when singularity is approached, and k_0 is the scale factor at singularity.

Weighted Least Norm solution proposed by [10] can be integrated to the control algorithm to optimize for secondary tasks. In order to put a motion preference of one joint rather than the other (such as the wheelchair wheels and the arm joints), a weighted norm of the joint velocity vector can be defined as:

$$|V|_w = \sqrt{V^T W V} \quad (7)$$

where W is a 9x9 symmetric and positive definite weighting matrix, and for simplicity, it can be a diagonal matrix that represent the motion preference of each joint of the system. For the purpose of analysis, the following transformations are introduced:

$$J_w = J W^{-1/2}, \text{ and } V_w = W^{-1/2} V \quad (8)$$

Using (5), (7) and (8), it can be shown that the weighted least norm solution integrated to the S-R inverse is:

$$|V|_w = W^{-1} J^T (J W^{-1} J^T + k * \underline{I}_6)^{-1} \dot{r} \quad (9)$$

The above method has been used in simulation of the 9-DoF WMRA system with the nine control variables (V) that represent the seven joint velocities of the arm and the linear and angular wheelchair's velocities. An optimization of criteria functions can be accomplished when used in the weighting matrix W .

C. Secondary trajectory planning

For the completion of an activity of daily living, the main task will be given as a set of trajectories for the end-effector to follow. Although the main task is followed, wheelchair position and orientation can be important for the task to be successfully completed. A secondary subtask representing the best position and orientation of the wheelchair is

represented as a secondary set of trajectories for the wheelchair to follow. An optimal position/orientation combination of the non-holonomic motion of the wheelchair can be achieved if the secondary trajectory is divided into 3 stages. The first one is to orient the wheelchair facing its desired linear trajectory. The second stage is to proceed with a linear motion along the secondary trajectory to approach the final planar coordinates. Once the wheelchair reaches its final position, the third stage will be to orient the wheelchair to its final desired orientation. Figure 2 shows the three stages implemented for the secondary trajectory.

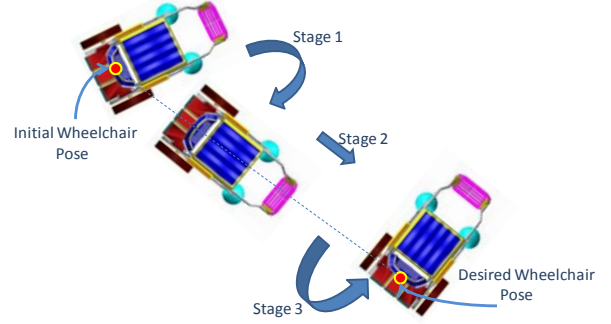


Figure 2. A general case of the three stages for the secondary trajectory to be followed by the wheelchair

The three stages to be applied for the secondary trajectory will only involve the position “ X ” and orientation “ φ ” variables of the wheelchair. As shown in figure 3, knowing the initial and final transformations of the wheelchair base, the trajectory angle α can be defined as:

$$\alpha = \tan^{-1} \left[\frac{(y_f - y_i)}{(x_f - x_i)} \right] \quad (10)$$

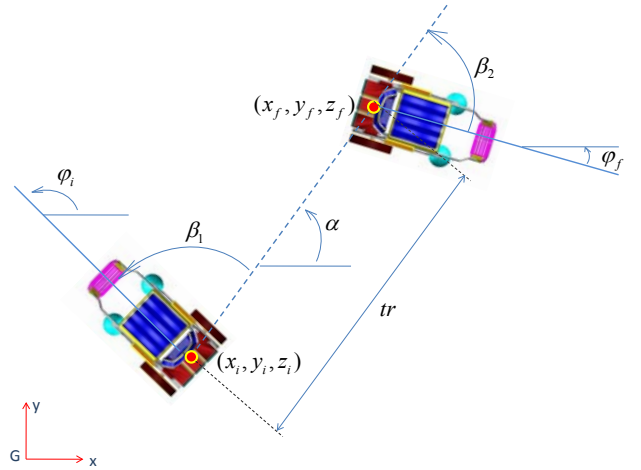


Figure 3. Definition of the optimization variables

That defines the amount of motion needed for the three stages to be followed in the following order:

- 1) Rotation by the amount of $\beta_1 = \alpha - \varphi_i$
- 2) Translation by the amount of $tr = \sqrt{(x_f - x_i)^2 + (y_f - y_i)^2}$
- 3) Rotation by the amount of $\beta_2 = \varphi_f - \alpha$

The above three wheelchair motion values can be utilized in the weight matrix as criteria to enforce the wheelchair motion.

D. Criteria functions for weighted optimization

The criteria functions used in the weight matrix for optimization can be defined based on different requirements. For the robotic arm, the physical joint limits can be avoided by minimizing an objective function that represents this criterion. One of these mathematical representations was proposed by [10] as follows:

$$H(q) = \sum_{i=1}^7 \frac{1}{4} \cdot \frac{(q_{i,\max} - q_{i,\min})^2}{(q_{i,\max} - q_{i,\text{current}}) \cdot (q_{i,\text{current}} - q_{i,\min})} \quad (11)$$

where “ q_i ” is the angle of joint “ i ”. This criterion function becomes “1” when the current joint angle is in the middle of its range, and it becomes “infinity” when the joint reaches either of its limits. The gradient projection of the criterion function can be defined as:

$$\frac{\partial H(q)}{\partial q_i} = \frac{(q_{i,\max} - q_{i,\min})^2 \cdot (2 \cdot q_{i,\text{current}} - q_{i,\max} - q_{i,\min})}{4 \cdot (q_{i,\max} - q_{i,\text{current}})^2 \cdot (q_{i,\text{current}} - q_{i,\min})^2} \quad (12)$$

When any particular joint is in the middle of the joint range, (12) becomes zero for that joint, and when it is at its limit, (12) becomes “infinity”, which means that the joint will carry an infinite weight that makes it impossible to move any further.

For the wheelchair, the criteria functions can be defined for each stage of its trajectory based on the desired motion of the wheelchair. Similar to the arm, mathematical representations can be obtained by treating the range of desired wheelchair motion as a motion limit. The upper limit in this case is set to be the current initial orientation (or position for the second trajectory stage) of the wheelchair. The lower limit is set to be double the rotation angle β_1 or β_2 (or double the translation distance tr for the second trajectory stage). In this case, the middle of that range will be the desired orientation/position of the wheelchair, and either limit will be avoided. Figure 4 shows an example of the limits for the first wheelchair trajectory stage.

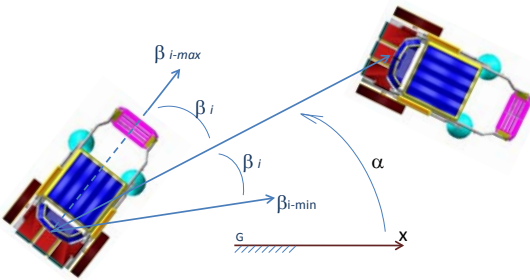


Figure 4. Gradient variable limits for the first wheelchair trajectory stage

To generalize the representation of the objective function, let variable “ P ” be a representative for β_1 , β_2 or tr . The objective function in this case is:

$$L(P) = \frac{1}{4} \cdot \frac{(P_{\max} - P_{\min})^2}{(P_{\max} - P_{\text{current}}) \cdot (P_{\text{current}} - P_{\min})} \quad (13)$$

and the gradient of the criterion function can be defined as:

$$\frac{\partial L(P)}{\partial P} = \frac{(P_{\max} - P_{\min})^2 \cdot (2 \cdot P_{\text{current}} - P_{\max} - P_{\min})}{4 \cdot (P_{\max} - P_{\text{current}})^2 \cdot (P_{\text{current}} - P_{\min})^2} \quad (14)$$

For the first stage, when the wheelchair’s angle is in the

middle of its allowable range, (14) becomes zero, and when it is at its limit, (14) becomes “infinity”, which means that the variable will carry an infinite weight that makes it impossible to move any further. This value of the gradient will be placed at the translational part of the weight matrix. The rotational part on the other hand will start with a very low value for (14). This way, rotational motion in the first stage will be active (with small weight), and the translational motion will be inactive (with high weight). The diagonal weight matrix W can then be constructed as:

$$W = \begin{bmatrix} w_1 + \left| \frac{\partial H(q)}{\partial q_1} \right| & 0 & \dots & \dots & 0 \\ 0 & w_2 + \left| \frac{\partial H(q)}{\partial q_2} \right| & 0 & \dots & 0 \\ \vdots & 0 & \ddots & \dots & \vdots \\ \vdots & \vdots & \vdots & w_x + \left| \frac{\partial L(X)}{\partial X} \right| & 0 \\ 0 & 0 & \dots & 0 & w_\phi + \left| \frac{\partial L(\beta)}{\partial \beta} \right| \end{bmatrix} \quad (15)$$

where for stages 1 and 3:

$$\frac{\partial L(\beta)}{\partial \beta} = \frac{(\beta_{\max} - \beta_{\min})^2 \cdot (2 \cdot \beta_{\text{current}} - \beta_{\max} - \beta_{\min})}{4 \cdot (\beta_{\max} - \beta_{\text{current}})^2 \cdot (\beta_{\text{current}} - \beta_{\min})^2}, \beta_{\min} < \beta < \beta_{\max}$$

$$\frac{\partial L(X)}{\partial X} = \frac{(X_{\max} - X_{\min})^2 \cdot (2 \cdot X_{\text{current}} - X_{\max} - X_{\min})}{4 \cdot (X_{\max} - X_{\text{current}})^2 \cdot (X_{\text{current}} - X_{\min})^2}, |X| < \text{tol}$$

$$\text{At the start of these stages } \left| \frac{\partial L(X)}{\partial X} \right| = \infty \text{ and } \left| \frac{\partial L(\beta)}{\partial \beta} \right| = 0$$

And for stage 2:

$$\frac{\partial L(\beta)}{\partial \beta} = \frac{(\beta_{\max} - \beta_{\min})^2 \cdot (2 \cdot \beta_{\text{current}} - \beta_{\max} - \beta_{\min})}{4 \cdot (\beta_{\max} - \beta_{\text{current}})^2 \cdot (\beta_{\text{current}} - \beta_{\min})^2}, |\beta| < \text{tol}$$

$$\frac{\partial L(X)}{\partial X} = \frac{(X_{\max} - X_{\min})^2 \cdot (2 \cdot X_{\text{current}} - X_{\max} - X_{\min})}{4 \cdot (X_{\max} - X_{\text{current}})^2 \cdot (X_{\text{current}} - X_{\min})^2}, X_{\min} < X < X_{\max}$$

$$\text{At the start of stage 2 } \left| \frac{\partial L(X)}{\partial X} \right| = 0 \text{ and } \left| \frac{\partial L(\beta)}{\partial \beta} \right| = \infty$$

where w_i is a user-set preference value for each joint and the position/orientation of the wheelchair. These values can achieve the user preference if joint limits are not approached and wheelchair motion is at its desired position.

This procedure can achieve the desired trajectory combinations to successfully execute tasks that require separate end-effector and wheelchair trajectories. An example of ADL task was tested in simulation and the results will be presented in the next section.

IV. RESULTS

To illustrate the simulation, a virtual reality WMRA environment was developed for several activities of daily living [17]. In this paper, a “Go To and Open the Door” task was selected to proof the concept. For illustration purposes the initial and final transformations of the end-effector trajectory are known. The initial and final transformations of the wheelchair approach trajectory are also given.

The task process is divided into two sub-tasks. The first task is to approach the door knob while both the end-effector and the wheelchair are following their respective trajectories. In this sub-task, the end-effector follows its straight-line trajectory from start to end, and the wheelchair follows the three stages of its trajectory to approach the door approximately at the desired position and orientation. The second sub-task is to open the door inwards while the wheelchair is backing up away from the door. In this sub-task, the end-effector follows its circular trajectory to open the door, and the wheelchair follows a single-stage straight-line trajectory to back up away from the door. The wheelchair orientation during this sub-task is kept constant.

Figure 5 shows the complete task execution; reaching the door and following a circular path to open it. In that sequence, the transition between figures 5-I and 5-II shows how the end-effector was following its 3D trajectory while the wheelchair was rotating without translation to reach its trajectory orientation. After reaching an approximate angle equivalent to that of the trajectory line, the wheelchair started moving forward without rotation, while the end-effector was still following its trajectory as shown in figures 5-III and 5-IV. The transition between figures 5-IV and 5-V shows how the end-effector kept following its 3D trajectory while the wheelchair was rotating back without translation to the desired orientation.

Figure 5-VI shows the end-effector following the circular trajectory to open the door, and the wheelchair was moving backwards to clear the space for the door to open. Figures 5-VII and 5-VIII show the completed task of opening the door and arriving at the final pose. Notice here that a third sub-task can be added to have the WMRA go through the door. In that case, the end-effector will need to stay stationary while the wheelchair moves forward to go through the door.

Note that the secondary trajectory will not be followed in a precise motion. As the weights of the wheelchair position and orientation are updated at every iteration in the weight matrix, the relative motion is kept to minimum for the undesired variable motion, while the relative motion of the desired variable is kept to maximum. Figures 6 and 7 show the resulting wheelchair motion in its three position/orientation stages for the first sub-task of approaching the door. In figure 6, it can be seen that the position stayed close to its desired trajectory throughout the wheelchair motion. Orientation, however, seems to have slightly higher error in following its desired orientation as seen in figure 7. In some extreme cases, fail can occur when this algorithm is used due to the fact that it is impossible to achieve both trajectories at the same time. An example of that is when the end-effector is commanded to go in a

direction that is deviating away from the desired wheelchair direction.

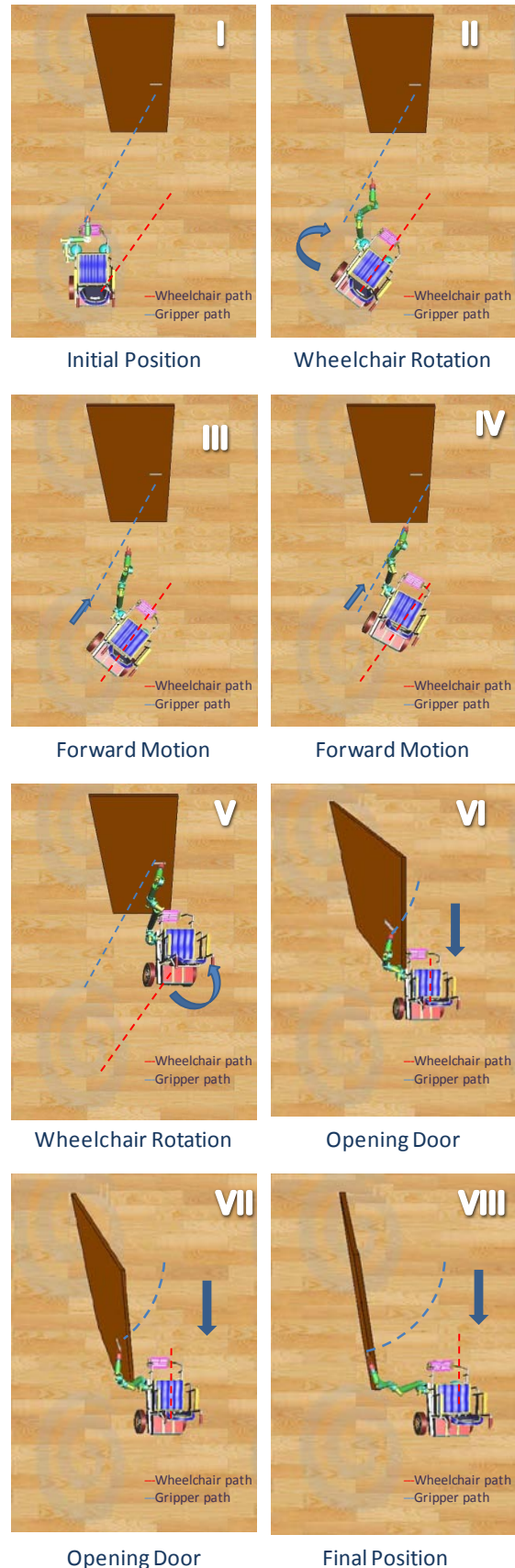


Figure 5. VR simulation sequence for sample task

It is shown, however, that even if the sub-task that is being performed by the wheelchair fails at certain instances, the trajectory-following of the end-effector stays unaffected.

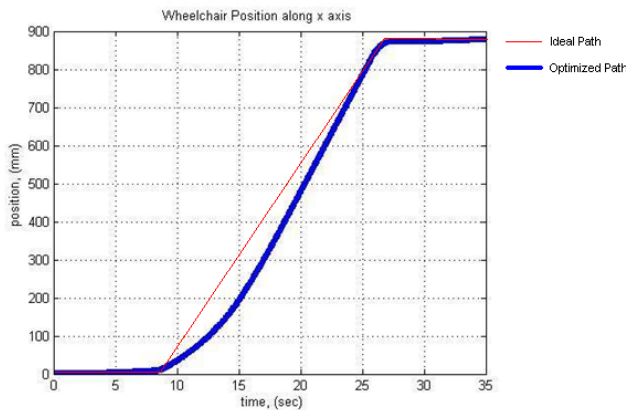


Figure 6. Wheelchair position vs. time for approaching task

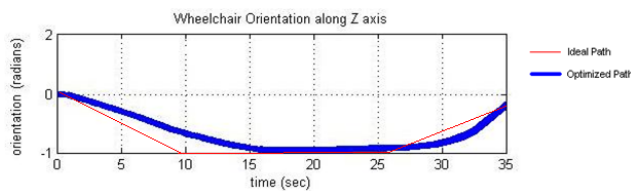


Figure 7. Wheelchair Orientation vs. time for approaching task

This example assumes that the door opens towards the wheelchair and towards the left side of the user as shown in figure 5. If the door opens to the right side of the user while the robotic arm is mounted on the left side of the user, a more complicated trajectory is required to achieve acceptable results. Programming several sequences of trajectories for both the wheelchair and the end-effector can be utilized to form a complete set of tasks that can be autonomously preformed to make the WMRA system a task-oriented system.

V. CONCLUSIONS AND FUTURE WORK

Optimized dual-trajectory following control system was presented for a 9-DoF redundant wheelchair-mounted robotic arm system to be used for people with disabilities to help them in their ADL tasks. S-R inverse was used with a weighting matrix to solve for the resolved rate solution to follow a primary trajectory. A secondary trajectory for the wheelchair to follow was mathematically represented and implemented for a “Go To and Open the Door” task. Joint limits for the manipulator joint variables and the position/orientation variables for the wheelchair were used in the weight matrix to prioritize or penalize the motion of the nine control variables. A simulation of the task was presented in virtual reality simulation, and the results were presented. Although these results are presented in simulation, ongoing efforts will test human subjects in simulation and in the physical system. These results are intended for future publications. More complicated environments will also be simulated and tested.

Future work includes the addition of a pool of ADL tasks in the program and the incorporation of a laser range finder

to obtain position information of the target and the environment. Implementation of the control system will be done in the new prototype WMRA under development. Clinical human testing of actual ADL tasks will follow, and data will be collected and presented in future publications.

VI. REFERENCES

- [1] US Census Bureau, “Americans with disabilities: 2002,” Census Brief, May 2006, <http://www.census.gov/prod/2006pubs/p70-107.pdf>
- [2] Reswick J.B., “The moon over dubrovnik - a tale of worldwide impact on persons with disabilities,” *Advances in External Control of Human Extremities*, 1990.
- [3] R. Alqasemi and R. Dubey. “Maximizing Manipulation Capabilities for People with Disabilities Using a 9-DoF Wheelchair-Mounted Robotic Arm System”. *Proceedings of the 2007 IEEE 10th International Conference on Rehabilitation Robotics*.
- [4] P. Shrock, F. Farello, R. Alqasemi and R. Dubey. “Design, Simulation and Testing of a New Modular Wheelchair Mounted Robotic Arm to Perform Activities of Daily Living” *Proceedings of the 2009 IEEE 11th International Conference on Rehabilitation Robotics*.
- [5] C. Ding, P. Duan, M. Zhang and H. Liu. “The Kinematics of a Redundant Mobile Manipulator”, *Proceedings of the IEEE International Conference on Automation and Logistics*. 2009.
- [6] A. Luca, G. Oriolo, and P. Giordano, “Kinematic Modeling and Redundancy Resolution for Nonholonomic Mobile Manipulators”, *Proceedings of the 2006 IEEE International Conference on Robotics and Automation (ICRA)*, pp. 1867-1873.
- [7] R. Zapata, JB. Thevenon, M. Perrier, E. Pommier and E. Badi. “Path Planning and trajectory Planning for Non-holonomic Mobile Robots”, *IEEE/RJS International Workshop on Intelligent Robot and Systems*. 1989
- [8] O. Gal, Z. Shiller and E. Rimon. “Efficient and Safe On-line Motion planning in Dynamic Environments”, *Proceedings of the 2009 IEEE International Conference on Robotics and Automation (ICRA)*.
- [9] G.D. white, R.M. Bhatt, C. Pei Tang and V.N. Krovi. “Experimental Evaluation of Dynamic redundancy resolution in a Nonholonomic wheeled Mobile Manipulator”. *IEEE/ASME Transactions on Mechatronics*, Vol. 14, No 3. 2009
- [10] T. Chan, and R. Dubey, “A Weighted Least-Norm Solution Based Scheme for Avoiding Joint Limits for Redundant Joint Manipulators”, *IEEE Robotics and Automation Transactions (R&A Transactions)*, V. 11, N. 2, pp. 286-292, 1995.
- [11] R. Alqasemi. “Maximizing Manipulation Capabilities for People with Disabilities Using a 9-DoF Wheelchair-Mounted Robotic Arm System”. *Doctoral Dissertation*. University of South Florida. Tampa, 2007.
- [12] E. Papadopoulos, J. Poulakakis, “Planning and model-based control for mobile manipulators,” *Proceedings of the 2001 IROS*, 2000
- [13] R.M. Alqasemi, E.J. McCaffrey, K.D. Edwards, R.V. Dubey, “Analysis, evaluation and development of wheelchair-mounted robotic arms,” *Proceedings of the 2005 ICORR*, Chicago, IL, June 2005.
- [14] Craig, J., 2003, “Introduction to robotics mechanics and control”, third edition, Addison- Wesley Publishing, ISBN 0201543613.
- [15] Nakamura, Y., “Advanced robotics: redundancy and optimization,” Addison- Wesley Publishing, 1991, ISBN 0201151987.
- [16] Yoshikawa, T., “Foundations of robotics: analysis and control,” MIT Press, 1990, ISBN 0262240289.
- [17] F. Farello, R. Alqasemi and R. Dubey. “Development of a Virtual Reality Environment for the Simulation of a Wheelchair Mounted Robotic arm Performing Activities of Daily Living”, *3rd International Congress of Mechanical Engineering (Tercer Congreso Internacional de Ingenieria Mecanica –Spanish)*. Barranquilla, Colombia. 2009.